Coarsening in the q-state Potts model and the Ising model with globally conserved magnetization

Clément Sire[1,*] and Satya N. Majumdar[2,†]
[1]*Laboratoire de Physique Quantique, URA 505 du CNRS, Université Paul Sabatier, 31062 Toulouse Cedex, France*
[2]*Department of Physics, Yale University, New Haven, Connecticut 06511*
(Received 18 November 1994)

We study the nonequilibrium dynamics of the q-state Potts model following a quench from the high-temperature disordered phase to zero temperature. The time-dependent two-point correlation functions of the order parameter field satisfy dynamic scaling with a length scale $L(t) \sim t^{1/2}$. In particular, the autocorrelation function decays as $[L(t)]^{-\lambda(q)}$. We illustrate these properties by solving exactly the kinetic Potts model in $d=1$. We then analyze a Langevin equation of an appropriate field theory to compute these correlation functions for general q and d. We establish a correspondence between the two-point correlations of the q-state Potts model and those of a kinetic Ising model evolving with a fixed magnetization $(2/q-1)$. The dynamics of this Ising model is solved exactly in the large q limit and in the limit of a large number of components n for the order parameter. For general q and in any dimension, we introduce a Gaussian closure approximation and calculate within this approximation the scaling functions and the exponent $\lambda(q)$. These are in good agreement with the direct numerical simulations of the Potts model as well as the kinetic Ising model with fixed magnetization. We also discuss the existing and possible experimental realizations of these models.

PACS number(s): 05.70.Ln, 05.40.+j, 82.20.−w

I. INTRODUCTION

Coarsening of domains of equilibrium ordered phases, following a quench from the disordered homogeneous phase to a regime where the system develops long-range order, is widely observed in many physical systems such as binary alloys, liquid crystals, magnetic bubbles, Langmuir films, and soap bubbles [1,2]. After the quench, domains of the different ordered phases form and grow with time as the system attains local equilibrium on larger and larger length scales. A dynamic scaling hypothesis suggests that at late times the system is left with a single length scale (linear size of a typical domain) that grows with time as $L(t) \sim t^n$, where n depends on the conservation laws satisfied by the dynamics [1,2]. For systems with only two types of ordered phases (such as a binary alloy or the Ising model), the nonequilibrium coarsening dynamics have been extensively studied experimentally, numerically, and by approximate analytical methods. Comparatively, much less is known when there are more than two ordered phases. A particular example of the latter class of models is the q-state Potts model, which has q ordered phases [3]. For $q=2$, this corresponds to the Ising model and there are experimental realizations also for $q=3,4,\infty$ [3]. As q increases, the morphology of the coarsening patterns changes from one of large connected interpenetrating domains to one of more and more isotropic droplets. The limit $q \to \infty$ is known to correctly describe the evolution of a dry soap froth and the growth of metallic grains [4]. The reason for taking $q=\infty$ is to prevent bubbles represented by different Potts indices from coalescing. In a way, a finite but large q Potts model describes a froth in which wall breakage occurs with a probability of order $1/q$ (Fig. 1).

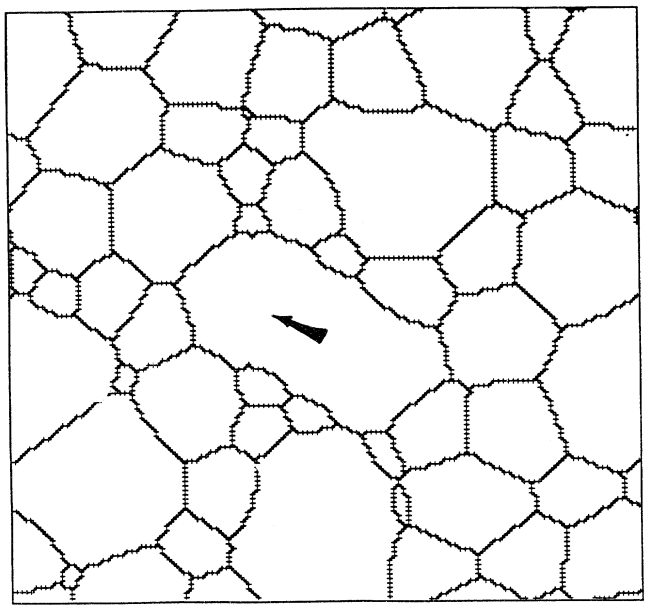

FIG. 1. Late-time configuration for $q=30$ fields evolving according to Eq. (5.2). Note the bubble marked by an arrow, which is highly nonisotropic, resulting from the coalescence of two bubbles with the same index.

*Electronic address: clement@siberia.ups-tlse.fr
†Electronic address: satya@cmphys.eng.yale.edu

Most studies of soap bubbles have so far focused on geometrical properties of the froth. For instance, mean-field treatments [5,6] and numerical simulations [4], as well as experiments [7], have addressed issues such as the joint distribution of bubble area and coordination number. However, while in other physical problems of coarsening the dynamic scaling and the correlation functions have been of central interest, no theoretical analysis exists of spatial and temporal correlations in a froth.

For the Potts model with finite q, there have been only numerical studies of the growth law of domains, confirming $L(t) \sim t^{1/2}$ [4,8] and substantiating the scaling of the equal-time correlation function [8]. However, to our knowledge, the two-time correlation has never been studied previously, not even numerically. In this paper, following our recent Letter [9], we show that the autocorrelation $A(t) = \langle \phi(\mathbf{r},0)\phi(\mathbf{r},t) \rangle$, measuring the correlation of the order parameter field $\phi(\mathbf{r},t)$ with its initial value $\phi(\mathbf{r},0)$, decays as $A(t) \sim [L(t)]^{-\lambda(q)}$. Thus, while the growth exponent remains $\frac{1}{2}$ for all q, the autocorrelation exponent depends explicitly on q. In [9], we established a correspondence between the dynamics of the q-state model and that of a kinetic Ising model evolving with a fixed magnetization $(2/q-1)$. In the present work, we explore more of this correspondence and derive several results.

For $q=2$, the Potts model is by definition identical to the Ising model. For $q>2$, our correspondence makes contact between the kinetic Potts model and a kinetic Ising model evolving with a fixed magnetization. This is useful not only because Ising models are conceptually much easier to think about, but also due to the fact that they are much easier to access experimentally, especially for the measurement of nonequilibrium dynamical properties. For example, in a recent experiment using video microscopy [10], the autocorrelation exponent has been measured for a liquid crystal sample confined between two parallel plates. The plates were designed such that molecules were bound to align along two perpendicular directions at the surface of the two plates. The two directions of the "helix" described by the molecules between the two plates (clockwise or counterclockwise) then represent the two possible "spin" states. This system then obeys Ising symmetry in $d=2$ and corresponds to $q=2$ (fixed 50%-50% mixture of "up" and "down" phases). The experimentally measured autocorrelation exponent $\lambda_{\text{expt}} = 1.246 \pm 0.079$ [10] is in good agreement with the numerical simulation of the $d=2$ kinetic Ising model $\lambda_{\text{num}} = 1.25 \pm 0.01$ [11] (see also Sec. VI). In Ref. [11], it was also argued heuristically that $\lambda = \frac{5}{4}$ for $d=2$. The Gaussian closure approximation (GCA) for $q=2$ leads to $\lambda_{\text{GCA}} \approx 1.286$ [12] (see also Sec. V). In principle, for other values of q, $\lambda(q)$ could be measured in such a system if one succeeds in maintaining a fixed concentration of up phase, different from 50%.

For $q>2$, exploiting our correspondence to an Ising model, another possible experimental system for measuring $\lambda(q)$ might be magnetic bubbles [13,14]. Magnetic bubbles are a natural realization of the kinetic Ising model where increasing the magnetic field leads to the coarsening of the system. In principle, $\lambda(q)$ could be measured if a constant magnetization path in the phase diagram is chosen [14]. Note that in order to determine $\lambda(q)$, the "real-time" scale, which, as already mentioned, is mapped onto a function of the magnetic field in this system, is not explicitly needed since the definition of $\lambda(q)$ only involves the domains length scale $L(t)$.

The paper is organized as follows. In Sec. II we solve exactly the dynamics of the $d=1$ q-state Potts model and compute the equal-time and the two-time correlation functions. We find $\lambda(q,d=1)=1$ for all q and show that this problem is equivalent to the $d=1$ Glauber dynamics for the Ising model with constant magnetization $m_0 = 2/q-1$. In Sec. III we present an exact theory of the coarsening of this Ising model with globally conserved magnetization $m_0 = 2/q-1$, in the $q \to \infty$ limit, and in any dimension $d>1$. The distribution of droplet radii and the equal-time correlation functions are computed exactly and we find $\lambda(q=\infty,d)=d$. Section IV is devoted to the exact solution of an $O(n)$ model evolving with a globally conserved magnetization, in the $n \to \infty$ limit. The correlation functions are again calculated and $\lambda(q,n=\infty,d)=d/2$. In Sec. V, we first establish a general correspondence between the dynamics of the q-state Potts model and that of the Ising model evolving with a fixed magnetization $2/q-1$ and then present a nontrivial extension of the GCA [12] to this Ising model (a brief version of which was communicated earlier [9]). This approach gives very accurate results for general q and also reproduces the exact results obtained in the different limits mentioned above. Finally, in Sec. VI, we present extensive numerical simulations for the Potts and Ising models separately, which confirm the mentioned correspondence and show that the GCA is indeed remarkably accurate.

As a prelude to the following sections, we first define the Potts model Hamiltonian as [3]

$$\mathcal{H} = -\sum_{\langle ij \rangle} \delta_{\sigma_i \sigma_j} . \tag{1.1}$$

σ_i takes integer values $\sigma_i = 1, \ldots, q$. The sum is over nearest neighbors, but can be extended to the next shell of neighbors, as is needed in $T=0$ Monte Carlo simulations, in order to avoid pinning to the lattice (see Sec. VI).

II. q-STATE POTTS MODEL IN ONE DIMENSION

We now consider the zero temperature Glauber dynamics of the q-state Potts model in one dimension. Contrary to higher dimensions where the domain growth is driven by interfacial tension, coarsening in $d=1$ occurs via the diffusion and annihilation of kinks [Fig. 2(a)]. We start with a totally random initial condition where each of the q phases is present with equal density $c = 1/q$. The zero temperature dynamics proceeds as follows: a spin is selected at random and its value is changed to that of either of its neighbors with equal probability. It gives rise to three possible situations as shown in Fig. 2. We now focus on one particular phase with an arbitrary Potts index $\sigma = l$ and define an indicator function $\phi(x,t)$, which is

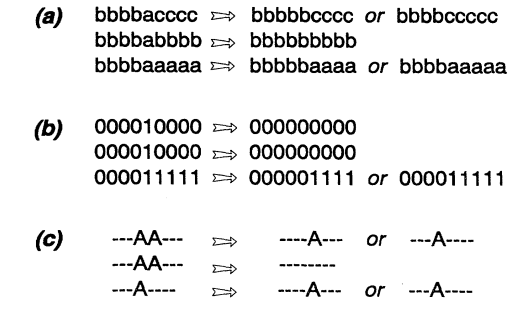

FIG. 2. Potts model in one dimension: (a) the three elementary dynamical flips of the central Potts spin with index a; (b) associating 1's to the a phase and 0's to the other phases, one obtains an effective Glauber dynamics; (c) associating a particle A to each interface, the model is mapped on a reaction diffusion model as described in the text.

1 if the site x is occupied by this lth phase and 0 otherwise. In this new two-phase system, the density of the 1's is $c=1/q$ and the 0's, representing the $(q-1)$ other phases, have a density $1-c$. For later convenience, we prefer the $\phi=0,1$ convention to the more usual spin representation $\phi=\pm 1$. The density c is related to the usual magnetization m_0 by the relation $m_0=2c-1$. Then the dynamics of ϕ is governed by the Glauber dynamics [15] of the Ising model with a constant magnetization $m_0=2/q-1$. This is illustrated in Fig. 2(b).

Using this mapping, the equal-time correlation function $G(r,t)=\langle\phi(r,t)\phi(0,t)\rangle$, in the scaling limit, is given by [15]

$$qG(r,t)=\left[1-\frac{1}{q}\right]\operatorname{erfc}\left[\frac{r}{2\sqrt{t}}\right]+\frac{1}{q}\ , \tag{2.1}$$

where $\operatorname{erfc}(x)=(2/\sqrt{\pi})\int_x^\infty \exp(-u^2)du$. We now point out that in the $q\to\infty$ limit this correlation function is related to the probability distribution of spacings between domain walls (kinks in $d=1$). The quantity $qG(r,t)$ measures the probability that the spins at 0 and r have the same value at time t. For finite q, this is different from the probability that they belong to the same domain. However, when $q\to\infty$, two spins that are equal are necessarily in the same domain (bubble). Then, $qG(r,t)$ is the probability of having a domain of length r or more. It is then a standard result that the normalized spacing distribution of kinks $P(r,t)$ is given by $P(r,t)=2qL(t)[\partial^2 G(r,t)/\partial r^2]$. For large times, this distribution also obeys scaling: $P(r,t)=[L(t)]^{-1}p(r/L(t))$, where

$$p(x)=\frac{\pi}{2}\left[\frac{1}{q-1}\right]^2 x\exp\left[-\frac{\pi}{4}\left[\frac{q}{q-1}\right]^2 x^2\right]\ .$$

This result, in the $q\to+\infty$ limit, was first obtained by Derrida, Godrèche, and Yekutieli by using an analogy to a random-walk problem [16]. Interestingly, this Wigner distribution is also identical to the eigenvalue spacing distribution for a real random Hermitian matrix [17].

We also note that this result coincides with the spacing distribution in the reaction diffusion model $A+A\to A$ [18]. This can be understood in the following way. Representing a kink by a particle A on a $d=1$ line, the dynamics of the Potts model can be mapped to that of a reaction diffusion model where the particles A diffuse, annihilate, and coagulate according to the following rules: Each particle undergoes diffusion until two of them meet, in which case they either annihilate $(A+A\to\varnothing)$ with probability $1/(q-1)$ or coagulate $(A+A\to A)$ with probability $(q-2)/(q-1)$ [see Fig. 2(c)]. For $q=2$, the particles only annihilate and hence this is equivalent to the Glauber model [15], whereas in the $q\to\infty$ limit they only coagulate. Both these limits have been studied previously [18,19]. In the Glauber case, the two-point correlation function has been calculated analytically, but the spacing distribution is still unknown. On the other hand, for the $A+A\to A$ model, the spacing distribution is known exactly, but there was no analogy to any spin model and hence correlation function. Our present result establishes that the dynamics of these two problems are two different solvable limits of that of the q-state Potts model.

We now consider the two-time correlation function $C(r,t)=\langle\delta_{\sigma(r,t),\sigma(0,0)}-1/q^2\rangle$. In terms of the indicator field ϕ, $C(r,t)=\langle\phi(r,t)\phi(0,0)-1/q^2\rangle$, which is expected to scale as $C(r,t)\sim[L(t)]^{-\lambda}c(r/L(t))$ [11]. Thus the autocorrelation $A(t)=C(0,t)$ decays as $A(t)\sim L(t)^{-\lambda}$, where λ is a nontrivial nonequilibrium exponent [11]. In $d=1$ and for all q, we find that $C(r,t)$ satisfies a diffusion equation and is given by $C(r,t)\sim t^{-1/2}\exp(-r^2/2t)$. Since the length scale $L(t)\sim t^{1/2}$, we establish the scaling of $C(r,t)$ and find $\lambda=1$ for all q. This is consistent with our general exact result that $\lambda=d$ in the $q\to\infty$ limit, as we argue in the following sections.

In one dimension, we have shown that the evolution of the two-point correlation functions in the kinetic Potts model can be exactly mapped to that of the Ising model with fixed magnetization $(2/q-1)$. In Sec. V, we will show that this correspondence essentially holds even in higher dimensions. This fact motivates us to study the dynamics of the Ising model evolving with fixed magnetization. In the following section, we show that this problem can be exactly solved in the $q\to\infty$ limit.

III. SMALL VOLUME FRACTION LIMIT

In this section, we study the coarsening of a magnetic system with *globally* conserved magnetization $m_0=(2/q-1)$, or equivalently with a density $c=1/q$ of the minority phase (up), in the $c\to 0$ limit. This becomes a modified version (suited for globally fixed magnetization) of the celebrated Lifshitz-Slyozov (LS) theory [20,21], which describes the coarsening of a two-phase system with *local* conservation (model B [22]). On a discrete lattice, both models are described by spin-exchange Kawasaki dynamics. However, in one case the exchange occurs between spins on any two arbitrary sites (global conservation) whereas in the other case, the exchange occurs only between two sites that are nearest neighbors to each other (local conservation). For $c=\frac{1}{2}$, the globally conserved model [hereafter called model

$A(c)$] has been shown to be in the same universality class as the standard model-A dynamics as far as the dynamical exponent and the domain growth exponent are concerned [23,24]. In Sec. VI, we will show that the autocorrelation exponent λ is also the same for a strict global $c=\frac{1}{2}$ conservation and for model A, namely, $\lambda \approx 1.25$. However, for $c<\frac{1}{2}$, we find (see Sec. VI) that λ is explicitly a function of c. At the end of this section, we show (within the framework of the LS theory, which is exact in the zero volume fraction limit) that $\lim_{c\to 0}\lambda(c)=d$. We recover this exact result also from our approximate treatment of the appropriate field theory (see Sec. V). This result is further verified from the direct numerical simulations (Sec. VI) of the q-state Potts model (large q limit) as well as the model $A(c)$.

In the $c\to 0$ limit, the coarsening pattern consists of circular bubbles that are growing or shrinking, but are always far apart from each other so that they never coalesce. A mean-field treatment assuming no correlation between these bubbles should then be exact in the limit $c\to 0$. In the following, we determine $N(R,t)$, the density of bubbles with radius r at time t.

The equation of motion for the radius $R_i(t)$ of bubble i is

$$\frac{dR_i}{dt}=-\frac{1}{R_i}+\lambda_1 . \tag{3.1}$$

The first term on the right-hand side, in which the surface-tension-dependent coefficient has been normalized to 1, contributes to making the bubble shrink, in order to minimize locally the interface length between the two phases. The second term $\lambda_1(t)$ is an effective time-dependent magnetic field, playing the role of a Lagrange multiplier (see Sec. V) fixing the constraint that $\sum_i R_i^d$ must be a constant proportional to cV, where V is the volume. Note that this equation of motion Eq. (3.1) can also be directly derived from the model-A equation of motion with this additional Lagrange multiplier needed to keep the magnetization fixed. The density $N(R,t)$ satisfies a continuity equation of the form

$$\frac{\partial N}{\partial t}+\frac{\partial}{\partial R}\left[\frac{dR}{dt}N\right] . \tag{3.2}$$

At late times we look for a scaling solution of the form $N(R,t)\approx[L(t)]^{-(d+1)}F(R/L(t))$, where $L(t)$ is proportional to the average radius of a growing bubble. The conservation law demands that the prefactor decays as $[L(t)]^{-(d+1)}$. Inserting Eq. (3.1) and the scaling form in Eq. (2.2), one easily sees that all terms are of the same order provided $L(dL/dt)$ is a constant, so that $L(t)\sim t^{1/2}$. Thus, in contrast to model-B dynamics where $L(t)\sim t^{1/3}$, model $A(c)$ has the same growth law as model A. We now set $L(dL/dt)=1$ and $\lambda_1(t)=\nu/L(t)$, where ν is to be determined by imposing that the solution of the scaling equation has physical limits. This form for λ_1 is justified by the fact that, in Eq. (3.1), λ_1 scales as R^{-1}. This fact will be physically justified in Sec. V in terms of balance between the interface and magnetic energies of a droplet. From now on, we present explicit results for $d=2$, but the generalization to $d>2$ is straightforward. The scaling function F then satisfies the differential equation

$$F'(x)=\frac{1-3x^2}{x(x^2-\nu x+1)}F(x) . \tag{3.3}$$

The condition that $F(x)$ goes to zero for large x demands that $\nu=2$, so that the function multiplying $F(x)$ in Eq. (3.3) has a double pole (at $x=1$). Then, solving this differential equation we get

$$F(x)=\begin{cases}\dfrac{A}{(1-x)^4}\exp\left[-\dfrac{2}{1-x}\right] & \text{for } x\le 1\\ 0 \quad \text{for } x\ge 1 ,\end{cases} \tag{3.4}$$

where the constant A is determined from the conservation condition. This scaling function is plotted in Fig. 3 and appears to be wider than the LS form for model B (local conservation) [25].

We now compute, in the limit $c\to 0$, the equal-time correlation function $G(r,t)=\langle\phi(r,t)\phi(0,t)\rangle/c$, where ϕ is the density field as defined in Sec. II. The function $G(r,t)$ can be computed from the normalized radius distribution function $N_0(R,t)=N(R,t)/\int \pi u^2 N(u,t)du = N(R,t)/cV$ in the following way. By definition,

$$G(r,t)=\frac{\int \phi(\mathbf{x}+\mathbf{r})\phi(\mathbf{x})d^2\mathbf{x}}{\int \phi(\mathbf{x})d^2\mathbf{x}}$$

$$=\frac{1}{cV}\sum_{i,j}\int \chi_i(\mathbf{x}+\mathbf{r})\chi_j(\mathbf{x})d^2\mathbf{x} , \tag{3.5}$$

where the indices i and j run over all the bubbles and $\chi_i(\mathbf{x})$ is the characteristic function of the ith bubble. In the $c\to 0$ limit, bubbles are strictly circular and $\chi_i(\mathbf{x})=\theta(R_i-|\mathbf{x}|)$, where θ is the usual step function and R_i is the radius of the ith bubble. In this low area fraction limit, the bubbles are far apart from each other and for finite r, only the terms corresponding to $i=j$ contrib-

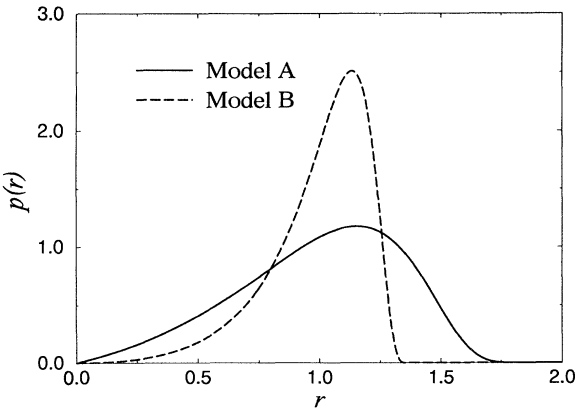

FIG. 3. Distribution of bubble radii for $d=2$ and model A, in the mean-field approximation [Eq. (3.4)], compared to the Lifshitz-Slyozov result for the locally conserved order parameter case (model B) [16,24]. Both distributions have been normalized and the r axis is scaled such that $\langle r\rangle=1$.

ute to the sum in Eq. (3.5). Then, we obtain the exact result in the $c \to 0$ limit

$$G(r,t)=\int dR\, N_0(R,t)\int d^2\mathbf{x}\,\chi_R(\mathbf{x}+\mathbf{r})\chi_R(\mathbf{x})\ . \quad (3.6)$$

The second integral is just the overlap area between two disks with radius R, with their centers separated by a distance r. The final expression is

$$G(r,t)=2\int_{r/2}^{+\infty} dR\, R^2 N_0(R,t) \times\left[\arccos\left[\frac{r}{2R}\right]-\frac{r}{2R}\left[1-\frac{r^2}{4R^2}\right]^{1/2}\right]. \quad (3.7)$$

In the scaling limit,

$$N_0(R,t)\approx\frac{1}{cV[L(t)]^3}F(R/L(t))\ ,$$

where $F(x)$ is given by Eq. (3.4), and therefore, from the above equation, we find explicitly that $G(r,t)\approx g(R/L(t))$. Thus dynamic scaling is established. The function $g(x)$ with x normalized such that $g(1)=\frac{1}{2}$ is shown in Fig. 4 and is seen to be in good agreement with large-q Potts model simulations and the field theory results presented below. Notice, however, that the mean-field equal-time correlation function has a finite support.

In the $c \to 0$ limit, it is also simple to calculate the autocorrelation exponent λ. Since bubbles do not coalesce in this limit and their centers do not diffuse, the autocorrelation $A(t)\approx\langle\phi(\mathbf{x},t)\phi(\mathbf{x},0)\rangle$ is essentially the survival probability of a bubble up to time t. After time t, the number of bubbles left is $N(t)=\int dR\, N(R,t)\sim[L(t)]^{-d}$ and therefore $\lambda=d$, in d dimensions. This result is confirmed by numerical simulations presented in Sec. VI.

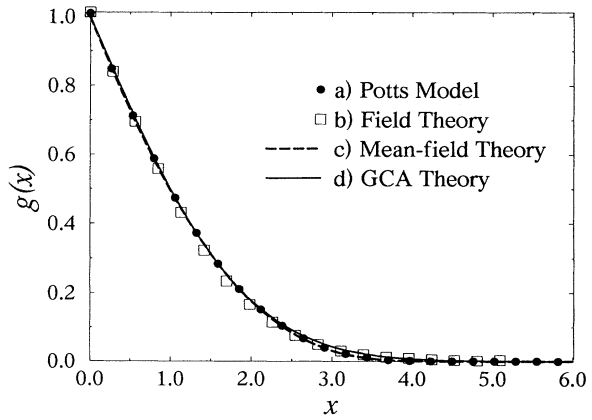

FIG. 4. Comparison of the scaled equal-time correlation functions generated by (a) numerical simulation of the Potts model with $q=\infty$ (in fact, q equals the initial number of bubbles $N_B\sim 32\,000$), (b) numerical integration of Eq. (5.2) with $q=50$ (symbols have the size of the typical error bars), (c) the mean-field theory of Sec. III [Eq. (3.7)], and (d) the large-q GCA analytical result of Sec. V.

IV. LARGE-n CALCULATION

Another example where the correlation functions (both equal-time and two-time) and the exponent λ can be calculated in the presence of a time-dependent magnetic field $\lambda_1(t)$ (to keep the average magnetization m_0 fixed) is the large n ($n\to\infty$) limit of the classical $O(n)$ vector model. The $O(n)$ model is described by an n component order parameter field $\vec{\phi}(\mathbf{r},t)=(\phi_1(\mathbf{r},t),\ldots,\phi_n(\mathbf{r},t))$ and a coarse-grained Landau-Ginzburg free-energy functional

$$\mathcal{H}(\vec{\phi})=\tfrac{1}{2}\int d^d\mathbf{r}\left[(\nabla\vec{\phi})^2+r_0\vec{\phi}^2+\frac{u}{2n}(\vec{\phi}^2)^2-2\lambda_1(t)\sum_\alpha\phi_\alpha\right], \quad (4.1)$$

where $\lambda_1(t)$ is a Lagrange multiplier to keep $(1/V)\sum_{\mathbf{r}}\phi_\alpha(\mathbf{r},t)$ fixed at $m_0=2/q-1$, where V is the system size. The model-A equation describing the overdamped relaxation is in general nonlinear and hard to solve. However, in the large n limit, this equation can be linearized in a self-consistent way [26] and therefore is exactly solvable in that limit. In Fourier space, this linearized equation (at $T=0$) reads

$$\frac{\partial\phi(\mathbf{k},t)}{\partial t}=-[k^2+r_0+uS_0(t)]\phi(\mathbf{k},t)+\lambda_1(t)\sqrt{V}\,\delta_{\mathbf{k}=0}\ , \quad (4.2)$$

where self-consistency for the structure factor demands that $S_0(t)=(1/V)\sum_{\mathbf{k}}S(\mathbf{k},t)$, where $S(\mathbf{k},t)=\langle\phi(\mathbf{k},t)\phi(-\mathbf{k},t)\rangle$. Note that $r_0<0$, since we are in the ordered phase. We have dropped the subscript α from ϕ_α since in the large n limit, the different components of $\vec{\phi}$ are completely uncorrelated with each other. The Lagrange multiplier $\lambda_1(t)$ is determined from Eq. (4.2) by demanding that $\phi(\mathbf{k}=0,t)=m_0\sqrt{V}$ and is given by $\lambda_1(t)=m_0[r_0+uS_0(t)]$. We use random initial conditions, for which $S(\mathbf{k},0)=\Delta-m_0^2$ or $\mathbf{k}\neq\mathbf{0}$, where Δ is of order unity and $S(\mathbf{k}=\mathbf{0},0)=m_0^2V$. Writing, $Q(t)=\int_0^t[r_0+uS_0(t')]dt'$, we get from Eq. (4.2), for $\mathbf{k}\neq\mathbf{0}$,

$$S(\mathbf{k},t)=(\Delta-m_0^2)\exp\{-2[k^2t+Q(t)]\}\ . \quad (4.3)$$

The self-consistency condition now reads

$$\frac{dQ}{dt}=r_0+um_0^2+\frac{u}{V}\sum_{\mathbf{k}}S(\mathbf{k},t)\ . \quad (4.4)$$

Plugging in the expression for $S(\mathbf{k},t)$ from Eq. (4.3) into Eq. (4.4) and taking the thermodynamic limit $V\to\infty$, we get

$$\frac{dQ}{dt}=r_0+um_0^2+u(\Delta-m_0^2)\Gamma t^{-d/2}\exp[-2Q(t)]\ , \quad (4.5)$$

where Γ is a constant that depends on the dimension d and the upper cutoff Λ of the theory. This equation is solved by making the ansatz $Q(t)=A+B\ln t$. The left-

hand side of Eq. (4.5) then decays as t^{-1}, whereas the leading-order term on the right-hand side is a constant. So, for consistency, one needs $B=-d/4$, so that the leading-order term on the right-hand side is identically zero. As a consequence, the structure factor for $\mathbf{k}\neq 0$ (Fourier transform of the equal-time correlation function) can be written in the form

$$S(\mathbf{k},t)\approx[L(t)]^{-d}s(\mathbf{k}L(t)) ,$$
$$\text{with } L(t)\approx t^{1/2} , \quad s(x)=C\exp(-2x^2) , \tag{4.6}$$

where C is a constant. We thus obtain the scaling of the correlation function with the expected domains length scale $L(t)\sim t^{1/2}$.

Similarly, the two-time correlation function $C(\mathbf{k},t)=\langle\phi(\mathbf{k},0)\phi(-\mathbf{k},t)\rangle$ for $\mathbf{k}\neq 0$ evolves as $C(\mathbf{k},t)=(\Delta-m_0^2)\exp\{-[k^2t+Q(t)]\}$. The autocorrelation function, defined as $A(t)=\langle\phi(\mathbf{r},0)\phi(\mathbf{r},t)\rangle-m_0^2$, then decays as $t^{-d/4}\sim L(t)^{-d/2}$. Thus the autocorrelation exponent is $\lambda=d/2$, as in the $m_0=0$ case [26]. This, however, is not unexpected because the limit $n\to\infty$ decouples the different $\mathbf{k}$ modes and the time-dependent magnetic field just couples to the $\mathbf{k}=\mathbf{0}$ mode, which has no effect on the evolution of the $\mathbf{k}\neq 0$ modes apart from modifying the prefactor. Therefore, in order to see the dependence of λ on m_0, one has to include the $O(1/n)$ corrections, which is a very difficult task [2].

V. FIELD THEORY AND GAUSSIAN CLOSURE APPROXIMATION

In our earlier Letter [9], we constructed a field theory of the q-state Potts model in terms of the coarse-grained "occupation density" fields $\{\phi_l(\mathbf{r},t);\, l=1,2,\ldots,q\}$ such that ϕ_l assumes that value 1 in the interior of the lth ordered phase and decays continuously to 0 outside. Consequently, inside any "bubble" of one phase, only one of the ϕ_l's is close to 1 and the others are all close to 0. We thus require a potential with q degenerate minima at $[1,0,0,\ldots,0],[0,1,0,\ldots,0],[0,0,0,\ldots,1]$, which prevents two different bubbles from sharing the same position in space. A suitable free-energy functional is [9],

$$\mathcal{F}[\{\phi_l\}]=\int d^d\mathbf{r}\left\{\sum_{l=1}^{q}\left[\tfrac{1}{2}(\nabla\phi_l)^2+V(\phi_l)\right]-\lambda_1\left[\sum_{l=1}^{q}\phi_l-1\right]+\lambda_2\left[\sum_{l=1}^{q}\left[\phi_l-\frac{1}{q}\right]^2-\frac{q-1}{q}\right]^2\right\} , \tag{5.1}$$

where $\lambda_1(\mathbf{r},t)$ is a Lagrange multiplier enforcing the constraint $\sum_l\phi_l=1$ and λ_2 is a constant ~ 1 such that the state $[1/q,\ldots,1/q]$ is unstable and $V(\phi)\sim\phi^2(1-\phi)^2$ is the usual double-well potential with minima at 0 and 1. Then, the equation of motion is

$$\frac{\partial\phi_l}{\partial t}=\nabla^2\phi_l-V'(\phi_l)+\lambda_1-4\lambda_2\left[\phi_l-\frac{1}{q}\right]\times\left[\sum_{l'=1}^{q}\left[\phi_{l'}-\frac{1}{q}\right]^2-\frac{q-1}{q}\right] \tag{5.2}$$

and $\lambda_1=(1/q)\sum_l V'(\phi_l)$ by demanding $\sum_l\phi_l=1$ in Eq. (5.2). Note that for $q=2$ (the Ising model), $\lambda_1=0$ by virtue of the condition $\phi_1+\phi_2=1$ and λ_2 can be chosen to be 0 since this term only renormalizes V. Then one recovers the usual time-dependent Landau equation for the Ising model. For $q>2$, we also note that this evolution equation has a form similar to that of Eq. (2.10) of Lau, Dasgupta, and Valls [8]. In Fig. 1, we show a late-time configuration of domains generated by Eq. (5.2) for $q=30$.

The two-point correlation function for the q-state Potts model is defined as $G(12)=\sum_{l=1}^{q}\langle\phi_l(\mathbf{r}_1,t_1)\phi_l(\mathbf{r}_2,t_2)\rangle$ and therefore equals $q\langle\phi_l(\mathbf{r}_1,t_1)\phi_l(\mathbf{r}_2,t_2)\rangle$ due to the symmetry between the q phases. Here, "12" is a shorthand notation for the pair of space-time points $(\mathbf{r}_1,t_1)$ and $(\mathbf{r}_2,t_2)$. Due to the isotropy and translation invariance in space, the only spatial dependence of these correlation functions is through $r=|\mathbf{r}_1-\mathbf{r}_2|$. Denoting the equal-time correlation function ($t_1=t_2=t$) by $G(r,t)$, we get from Eq. (5.2)

$$\frac{1}{2}\frac{\partial G}{\partial t}=\nabla^2G-q\langle\phi_1(0,t)[V'(\phi_l(\mathbf{r},t))-\lambda_1(\mathbf{r},t)]\rangle-4\lambda_2q\left\langle\phi_l(0,t)\left[\phi_l(\mathbf{r},t)-\frac{1}{q}\right]\left[\sum_{l'=1}^{q}\phi_{l'}^2(\mathbf{r},t)-1\right]\right\rangle . \tag{5.3}$$

Note that the two-time correlation function satisfies a similar equation.

Our first approximation is to replace $\sum_{l'}\phi_{l'}^2$ by its average $q\langle\phi_l^2\rangle=G(0,t)$ in the third term on the right-hand side of Eq. (5.3), which becomes exact in the $q\to\infty$ limit. Furthermore, the scaling solution $G(r,t)=g(r/L(t))$ must satisfy $g(0)=1$, so that we can drop the term $4\lambda_2[G(r,t)-1/q][G(0,t)-1]$ so produced. Thus the third term, although important in the evolution of ϕ_l since it provides stability to the bubbles, is not crucial in the evolution of the correlation functions, at least in the scaling limit of the large q model, but also for $q=2$ for which this term is simply absent. The two boundary conditions for $G(r,t)$ are (i) as $r\to 0$, $G(r,t)\to 1$ and (ii) as $r\to\infty$, $G(r,t)\to q\langle\phi_l(0,t)\rangle\langle\phi_l(\mathbf{r},t)\rangle=1/q$.

Next, using $\sum\phi_l(\mathbf{r},t)=1$, we get $\langle\sum\phi_l(\mathbf{r},t)\lambda_1(\mathbf{r},t)\rangle=\langle\lambda_1\rangle(t)$, and then, given the symmetry between the q phases, we can write $\langle\phi_l\lambda_1\rangle=(1/q)\langle\lambda_1\rangle=\langle\phi_l\rangle\langle\lambda_1\rangle$. Thus, without approximation, we replace in Eq. (5.3) $\lambda_1(\mathbf{r},t)$ by its average $\langle\lambda_1(\mathbf{r},t)\rangle$, which is simply a function of time. As a result, Eq. (5.3) reduces to an equation involving only a single field $\phi_l(\mathbf{r},t)$,

$$\frac{1}{2}\frac{\partial G}{\partial t}=\nabla^2G-q\langle\phi_l(0,t)[V'(\phi_l(\mathbf{r},t))-\langle\lambda_1\rangle]\rangle . \tag{5.4}$$

Interestingly, Eq. (5.4) is also the evolution equation for the two-point correlation in an Ising model evolving with fixed average magnetization $\langle m_0\rangle=2/q-1$ (equivalently, with a density of minority up spins fixed at $1/q$). The droplet domains of the minority phase in this Ising model would correspond to the bubbles of a particular phase in the Potts model, with the majority phase corresponding

to the remaining $(q-1)$ phases. $\langle\lambda_1\rangle$ acts as a time-dependent magnetic field, which prevents the minority phase from disappearing at $T=0$ and keeps the magnetization constant.

Thus, from now on, instead of the original Potts model, we consider the coarsening in the Ising model with globally conserved magnetization through a time-dependent magnetic field (Lagrange multiplier). The magnetization m_0 is related to the value of q of the Potts model via $m_0=2/q-1$.

The calculation of the two-point correlation function of this problem can be performed approximately by extending the Gaussian closure scheme as developed by Mazenko [12] for the usual Ising model where the magnetization remains fixed at $m_0=0$. The essence of this approximation scheme is to invoke an auxiliary field $m(\mathbf{r},t)$, which is related to the order parameter field $\phi(\mathbf{r},t)$ via a nonlinear transformation $\phi(\mathbf{r},t)=\sigma(m(\mathbf{r},t))$. The idea is to find a field $m(\mathbf{r},t)$, which varies smoothly across the interfaces, as opposed to the original field $\phi(\mathbf{r},t)$, which changes abruptly from nearly 0 to nearly 1 across an interface. So, the nontrivial part of the scheme is to choose the appropriate mapping function σ. In the case of the Ising model with zero magnetization, Mazenko argued that the function σ should be chosen as the equilibrium profile of ϕ near an interface, which is determined by the solution of

$$\frac{d^2\sigma}{dm^2}=V'(\sigma) \tag{5.5}$$

with the boundary conditions $\sigma(m)\to 1$ as $m\to+\infty$ and $\sigma(m)\to 0$ as $m\to-\infty$. The solution is $\sigma(m)=[1+\tanh(\beta m)]/2$, which at late times can be replaced by a step function, since domains grow [with $L(t)\sim t^{1/2}$] whereas the interface width ($\sim\beta^{-1}$ related to the coupling constant in front of V) remains bounded. The auxiliary field $m(\mathbf{r},t)$ can be interpreted as the distance from the nearest interface. The next part of the approximation is to assume that $m(\mathbf{r},t)$, being smooth across the interface, has a Gaussian distribution. The virtue of this "minimal" approximation is that it facilitates analytical calculation yielding nontrivial results for the correlation functions and the exponents, which are in good agreement with simulations, at least in the nonconserved case.

In order to extend this approximation to our problem with globally conserved magnetization, we start off with the assumption that there exists, as in the nonconserved Ising case, a nonlinear transformation $\phi(\mathbf{r},t)=\sigma(m(\mathbf{r},t),t)$ with a Gaussian auxiliary field. However, several important modifications need to be done in carrying out this extension from the simple Ising case. First, $\langle\phi(\mathbf{r},t)\rangle$ must be strictly fixed at $1/q$ at all times [by virtue of the time-dependent field $\langle\lambda_1\rangle(t)$], as opposed to the Ising case where, for a critical quench, $\langle\phi\rangle=\frac{1}{2}$ automatically. This also necessarily implies that the mean of the distribution of m is nonzero. The first and second moments of the Gaussian distribution, $\langle m(\mathbf{r},t)\rangle=\overline{m}(t)$ and $\langle\{m(\mathbf{r},t)-\overline{m}(t)\}^2\rangle=C_0(t)$ are space independent due to translational invariance. The complete correlation function $\langle\{m(\mathbf{r}_1,t_1)-\overline{m}(t_1)\}\{m(\mathbf{r}_2,t_2)-\overline{m}(t_2)\}\rangle=C(12)$ must be determined self-consistently as is $C(12)$ in the Ising case [12]. Now, from the condition $\langle\phi(\mathbf{r},t)\rangle=1/q$, we get

$$\frac{1}{\sqrt{2\pi C_0}}\int_{-\infty}^{\infty}\sigma(m)\exp[-(m-\overline{m})^2/2C_0]dm=1/q\ .$$

Replacing $\sigma(m,t)$ at late times by the step function $\theta(m)$ (which is 1 for $m>0$ and 0 for $m<0$), and thereby neglecting terms that are of lower order in t, we get $\overline{m}(t)=-\sqrt{2C_0(t)}\,\mathrm{erfc}^{-1}(2/q)$. Note that for $q=2$, $\overline{m}=0$ as expected. For later convenience, let us also define the correlation function $f(12)=C(12)/\sqrt{C_0(1)C_0(2)}$ and denote it by $f(\mathbf{r},t)$ when $t_1=t_2=t$. Note that $f(0,t)=1$, and $f\to 0$ as $r\to\infty$. Even for $t_1=t_2$, we will keep on writing $C_0(1)$ and $C_0(2)$ explicitly, although these two numbers are equal, since we will use formal derivatives with respect to $C_0(1)$.

The second important difference from the simple Ising case is the choice of the mapping function $\sigma(m(\mathbf{r},t),t)$. The explicit time dependence introduced via $\langle\lambda_1\rangle$ modifies the local equilibrium profile, thereby precluding the choice of the stationary profile $[1+\tanh(\beta m)]/2$. In fact, since the mean of the field $m(\mathbf{r},t)$ is time dependent [through $C_0(t)$, which scales linearly with t as we argue below], one can expect to get a "sigmoid" shaped solution only in a moving frame, with a velocity suitably determined to neutralize the time dependence introduced via $\langle\lambda_1\rangle$. Thus, making the transformation, $\mathbf{r}'=\mathbf{r}+a(t)\hat{\mathbf{n}}$, where $\hat{\mathbf{n}}$ is an arbitrary unit vector and $a(t)$ is to be determined, and demanding an equilibrium solution, i.e., $\partial\phi/\partial t=0$ to leading order in time, we find the appropriate equation for $\sigma(m,t)$,

$$\frac{d^2\sigma}{dm^2}+\frac{da}{dt}\frac{d\sigma}{dm}=V'(\sigma)-\langle\lambda_1\rangle\ . \tag{5.6}$$

We now fix $a(t)$ from the condition that the average value on both sides of Eq. (5.6) should be identical. The average on the right-hand side is zero by definition of $\langle\lambda_1\rangle$. Then, from Eq. (5.6), we get

$$\frac{da}{dt}=-\frac{\langle\sigma''(m)\rangle}{\langle\sigma'(m)\rangle}=-\frac{\int_{-\infty}^{+\infty}du\,\exp-\dfrac{(u-\overline{m})^2}{2C_0}\sigma''(u)}{\int_{-\infty}^{+\infty}du\,\exp-\dfrac{(u-\overline{m})^2}{2C_0}\sigma'(u)}\ . \tag{5.7}$$

Now $\langle d^2\sigma/dm^2\rangle/\langle d\sigma/dm\rangle$ is calculated by replacing $\sigma(m,t)$ by $\theta(m)$ at late times, so that $\sigma'(m)\approx\delta(m)$ and $\sigma''(m)\approx\delta'(m)$. This yields

$$\frac{da}{dt}\approx-\frac{d}{d\overline{m}}\ln\left[\exp-\frac{\overline{m}^2}{2C_0}\right]=\frac{\overline{m}}{C_0}\ . \tag{5.8}$$

Anticipating a scaling solution, we find that $a(t)\sim\sqrt{C_0(t)}\sim L(t)$, which is expected, since $L(t)$ is physically the only remaining length scale at late times. From Eq. (5.8) and the expression of $\overline{m}$ as a function of $C_0(t)$, we see that $\langle\lambda_1\rangle\sim[L(t)]^{-1}$, which can be understood on physical grounds: local equilibrium of a bubble and its interface requires that the surface tension energy

$E_S \sim [L(t)]^{d-1}$ should balance the magnetic energy $E_M \sim \langle \lambda_1 \rangle [L(t)]^d$ (see also Sec. III).

Using the fact that $m(\mathbf{r},t)$ has a Gaussian distribution, the correlation function $G(\mathbf{r},t)$ is given by

$$G(\mathbf{r},t)=\frac{q\gamma}{2\pi\sqrt{C_0(1)C_0(2)}}\int dx_1 dx_2 \sigma(x_1)\sigma(x_2)\exp\left[-\frac{\gamma^2}{2}\left[\frac{(x_1-\overline{m}_1)^2}{C_0(1)}+\frac{(x_2-\overline{m}_2)^2}{C_0(2)}-2(x_1-\overline{m}_1)(x_2-\overline{m}_2)\frac{f}{\sqrt{C_0(1)C_0(2)}}\right]\right], \tag{5.9}$$

where $\gamma=1/\sqrt{1-f^2}$ and we recall that $f(12)=C(12)/\sqrt{C_0(1)C_0(2)}$ and that the arguments 1 and 2 denote $(\mathbf{r},t)$ and $(0,t)$. The derivative with respect to m involved when inserting Eq. (5.6) in Eq. (5.4) are more easily expressed in the Fourier space associated with the variable x. $G(\mathbf{r},t)$ then takes the form

$$G(\mathbf{r},t)=\frac{q}{4\pi^2}\int dk_1 dk_2 \hat{\sigma}(k_1)\hat{\sigma}(k_2)\times\exp\left[-\frac{k_1^2}{2}C_0(1)-\frac{k_2^2}{2}C_0(2)-k_1k_2C(12)+ik_1\overline{m}_1+ik_2\overline{m}_2\right], \tag{5.10}$$

where $\hat{\sigma}$ is the Fourier transform of σ. From this expression one finds that

$$\left\langle\sigma(2)\frac{d^2\sigma}{dm^2}(1)\right\rangle=2\frac{\partial G}{\partial C_0(1)}\bigg|_{\overline{m}_1},\qquad \left\langle\sigma(2)\frac{d\sigma}{dm}(1)\right\rangle=\frac{\partial G}{\partial \overline{m}_1}\bigg|_{C_0(1)}. \tag{5.11}$$

Using this result and noting that for large time $\overline{m}_1/C_0(1)=2[\partial\overline{m}_1/\partial C_0(1)]$, the second term on the right-hand side of Eq. (5.4) can be written as

$$\left\langle\sigma(2)\frac{d^2\sigma}{dm^2}(1)\right\rangle+\frac{\overline{m}_1}{C_0(1)}\left\langle\sigma(2)\frac{d\sigma}{dm}(1)\right\rangle=2\left[\frac{\partial G}{\partial C_0(1)}\bigg|_{\overline{m}_1}+\frac{\partial\overline{m}_1}{\partial C_0(1)}\frac{\partial G}{\partial\overline{m}_1}\bigg|_{C_0(1)}\right]=2\frac{\partial G}{\partial C_0(1)}=-\frac{f}{C_0(1)}\frac{\partial G}{\partial f}. \tag{5.12}$$

Therefore, the evolution equation for the correlation function can be expressed as

$$\frac{1}{2}\frac{\partial G}{\partial t}=\nabla^2 G+\frac{1}{C_0(t)}Q(f), \tag{5.13}$$

where $Q(f)=f(\partial G/\partial f)$. Interestingly, we notice that Eq. (5.13) is identical in form to the Mazenko equation [12,9] for the critical Ising case with the exception that $G(f)$ has different expressions in the two cases. However, this seems accidental because in our problem we need to invoke a moving frame and therefore a different profile function satisfying Eq. (5.6). A naive application of the Mazenko theory with the mapping function determined by the equilibrium profile Eq. (5.5) leads to inconsistent and unphysical results. For $q=2$ ($c=\frac{1}{2}$, Ising critical), the velocity of the moving frame $da/dt \approx \overline{m}/C_0$ is zero identically and our expression then reduces to the Mazenko result.

Replacing σ by the θ function in Eq. (5.9), we get the leading term for $G(f)$ for large time:

$$G(f)=\frac{q}{\sqrt{\pi}}\int_0^\infty dy \exp\left\{-\left[y+p\left[\frac{2}{1+f}\right]^{1/2}\right]^2\right\}\times\operatorname{erf}\left[\left[\frac{1+f}{1-f}\right]^{1/2}y\right], \tag{5.14}$$

where $p=\operatorname{erfc}^{-1}(2/q)$. In principle, the function $G(f)$ can be inverted, so that Q is implicitly a function of G. Note that this function has the correct short [as $f\to 1$, $G(f)\to 1$] and long distance [as $f\to 0, G(f)\to 1/q$] behaviors. In addition, for $q=2$, it reduces to the Ising case [12], $G(f)=(2/\pi)\tan^{-1}[\sqrt{(1+f)/(1-f)}]$. We now substitute the scaling form $G(r,t)=g(r/L(t))$ in Eq. (5.13). A scaling solution is obtained provided $C_0(t)\sim[L(t)]^2\sim t$, which leads to the expected form for $L(t)$. The fact that $C_0(t)$ is proportional to $L^2(t)$ is consistent with the definition of $C_0(t)$ as a two-point correlation function of the field m, which has the physical meaning of a distance. The condition $L^2(t)\sim t$ is obtained by demanding that all terms in Eq. (5.13) obtained by plugging in a scaling form for the correlation function are of the same orders as a function of time. More precisely, setting $C_0(t)\approx 4t/\mu$ and $x=r/L(t)$, we get from Eq. (5.13),

$$\frac{d^2g}{dx^2}+\left[\frac{d-1}{x}+x\right]\frac{dg}{dx}+\mu Q(g)=0, \tag{5.15}$$

which defines a closed eigenvalue equation for the scaling function g. The eigenvalue μ has to be determined by matching the short and long distance behaviors of $g(x)$. The autocorrelation exponent λ is then related to μ via the relation $\lambda=d-\mu/2$, following an argument due to Mazenko [12] that we adapt to our problem below.

Following the same line of arguments as used to derive the evolution equation for G, we find that the two-time correlation function $C(\mathbf{r},t)=q\langle\phi(\mathbf{r},t)\phi(0,0)\rangle-q^{-1}$ satisfies the equation

$$\frac{\partial C}{\partial t}=\nabla^2 C+\frac{1}{C_0(r,t)}\hat{Q}(f), \tag{5.16}$$

where $\hat{Q}(f)=f(\partial C/\partial f)$ and $C(f)$ has the same f dependence as $G(f)$. Since the two-time correlation function decays with time, its value is very small at late times and then $Q\sim C$. With $C_0(t)\approx 4t/\mu$, this linear equation can be solved and $C(\mathbf{r},t)\sim t^{-(d/-\mu/2)/2}\exp(-\mathbf{r}^2/2t)$. Therefore, the autocorrelation $A(t)=C(0,t)\sim t^{-(d-\mu/2)/2}\sim[L(t)]^{-(d-\mu/2)}$ and $\lambda=d-\mu/2$.

In the $q\to\infty$ limit, it is possible to solve Eq. (5.15) analytically. Neglecting terms $\sim 1/p^4$ and using $\mathrm{erfc}(p)\sim\exp(-p^2)/p\sqrt{\pi}$ for large p, we find

$$g(f)\approx\frac{1+f}{2}\mathrm{erfc}\left[p\left[\frac{1-f}{1+f}\right]^{1/2}\right].$$

Note that as $f\to 0$, $g(f)=1/q+f(1+2p^2)/q+O(f^2)$, and as $f\to 1$, $g(f)\to 1-p\sqrt{2(1-f)}/\pi$. Then, expressing the function Q in terms of g itself, we find essentially three regimes. As $g\to 1/q$ (large distance), $Q(g)\approx g-1/q$, and as $g\to 1$ (short distance), $Q(g)\approx p^2/\pi(1-g)$. In the intermediate regime, $g^*\ll g\ll 1$, where $g^*\sim\ln(q)/q$, $Q(g)\approx p^2 g/2$. Note that, as q becomes larger and larger, the window over which $Q(g)$ behaves as $g-1/q$ becomes smaller and smaller and for a large range of distance one has $f\approx 1$. First consider the small x behavior of Eq. (5.15). Using $Q(g)\sim p^2/\pi(1-g)$, we find that $g(x)\to 1-p[\mu/\pi(d-1)]x$, reflecting the presence of sharp interfaces. This reproduces Porod's law [27], namely, that the structure factor scaling function $F(y)$, the Fourier transform of $g(x)$, decays as $y^{-(d+1)}$ for large argument y.

For very large q, since in the interesting range of distance one has $f(r,t)\approx 1$, one can find a very simple parameterization for g and $Q(g)$. Using the new variable $u\approx p(1-f)/2$, we obtain

$$\begin{aligned} g(u)&=\mathrm{erfc}(u)\ , \\ Q(u)&=p^2R(u)=\frac{p^2}{2\sqrt{\pi}u}\exp-u^2\ . \end{aligned} \tag{5.17}$$

Because of the overall factor p^2 in the expression of $Q(u)$ and since p grows with q [$p^2\approx\ln(q)$], we expect $\nu=\lim_{q\to\infty}\mu(q)p^2$ to be finite. Then, using the parameterization of Eq. (5.17), $u(x)$ satisfies the eigenequation

$$u''-2uu'^2+u'\left[\frac{d-1}{c}+x\right]-\frac{\nu}{4u}=0\ . \tag{5.18}$$

Porod's law gives $u\approx[\nu/2(d-1)]^{1/2}x$ for $x\to 0$ and the large x limit is easily found to be $u\approx/x/\sqrt{2}$. By matching the two regimes, one can check that $u(x)=x/\sqrt{2}$ is a solution of Eq. (5.15), provided the eigenvalue ν satisfies $\nu=2(d-1)$. The eigenfunction is then $g(x)=\mathrm{erfc}(x/\sqrt{2})$. Moreover, for large q, $\mu\sim 2(d-1)/p^2$, where $p^2\approx\ln(q)$ and therefore $\lambda\approx d-(d-1)/\ln q$.

We note that, for $d=1$, the eigenvalue problem can be solved directly for any q. The small x behavior of $g(x)$ obtained from Eq. (5.15) implies $\mu=0$. The scaling function then satisfies the differential equation $g''+xg'=0$. As a consequence, $g(x)$ coincides with the exact solution [Eq. (2.1)] of the $d=1$ q-state kinetic Potts model presented in Sec. II. $\mu=0$ leads to $\lambda=1$, which was also a result of the exact $d=1$ calculation. Thus the Gaussian closure approximation is exact in $d=1$.

VI. NUMERICAL SIMULATIONS

We now compare our results with the direct $T=0$ simulation of the q-state Potts model. We have also simulated directly our field theory [Eq. (5.2)] and found that it evolves in a way similar to the Potts model (see Fig. 1) with domains growing as $L^2(t)\sim t$. However, in the field theory, one needs as many fields (four bits real) as Potts indices, which limits the maximum lattice size ($\sim 120\times 120$), q ($q_{\max}\sim 50$), and the number of time steps. The determination of λ requires large lattice (especially for large q) and large numbers of Monte Carlo (MC) steps (typically 10^4 or more), which is easier to achieve in the Potts model simulation. The calculations have been carried out at $T=0$ on a 800×800 square lattice with equal coupling to nearest and next nearest neighbors. Next-nearest-neighbor interactions are needed at $T=0$ to avoid pinning to the lattice for $q>2$. It also ensures a better isotropy of surface tension and thus of bubbles. We optimize the MC procedure by only selecting surface Potts spins for updating, since only these can be flipped at $T=0$. For $q\le 20$, the results for 30–40 samples were averaged (more than in [9]), whereas 10–20 samples were bound to be sufficient for $q>20$, due to smaller fluctuations for $L(t)$ and $A(t)$ with increasing q, yielding, to our knowledge, the most extensive simulations to date.

We found $L^2(t)\sim t$ for all q, confirming a result already obtained in previous studies [4,8]. We also observed good scaling of the correlation functions. In Fig. 4 we compare the equal-time correlation function for $q\to\infty$ as given by the Potts model simulation, the direct simulation of the field theory for $q=50$ fields on a 120×120 lattice, the mean-field theory of Sec. III, and our approximate theory, and find good agreement between the numerical results and the two theoretical ones. For soap bubbles, $g(x)$ measures the probability that the point x belongs to the same bubble as the origin. Since bubbles are essentially isotropic, we expect g to be closely related to the distribution of radii. Since we find that $g(x)$ has a Gaussian tail, the distribution of areas ($A\sim x^2$) has a Poissonian tail. This result is consistent with a maximum entropy [28] and a mean-field [5,6] calculation. More precisely, the second derivative to $g(x)$ is proportional to the interface spacing distribution on a linear cut through the froth, which has a Wigner form [17] in our case.

A more interesting test of our theory concerns the computation of the autocorrelation exponent λ. The mean-field result of Sec. III predicts $\lambda=d$, whereas the large n calculation (Sec. IV) leads to $\lambda=d/2$. The more sophisticated Gaussian closure approximation of Sec. V gives less trivial and more accurate results: In Table I we present the values of λ generated in Potts simulations and compare them to those obtained from the (numerical) solution of the one-dimensional eigenvalue problem of Eq. (5.15). We find reasonably good agreement. Notice that for large q ($q>100$) the exponent λ obtained from Monte Carlo simulations is probably slightly overestimat-

TABLE I. λ for different q as computed from the Potts model simulation, for the globally conserved Ising model (see text), and by solving the eigenvalue equation (5.15) numerically.

q	2	10	20	30	50	100	200	$+\infty$
λ_{Potts}	1.25±0.01[a]	1.40±0.01	1.49±0.01	1.57±0.01	1.64±0.01	1.72±0.01	1.82±0.02	1.99±0.01
λ_{Ising}	1.25±0.01	1.40±0.01	1.48±0.02	1.55±0.02	1.61±0.02	1.70±0.02	1.84±0.02	–
λ_{theory}	1.289[b]	1.476	1.566	1.611	1.660	1.713	1.755	2.000

[a]See also Ref. [9].
[b]See also Ref. [15].

ed. This is due to the fact that for a finite lattice $q=\infty$ is actually realized for a finite value of q, so that one can expect that the effective number of different phase is $q_{\text{eff}}>q$. Finite size scaling indeed confirms this fact, although $\lambda(N)$ does not seem to have a simple form. In fact, for the values of q presented here, the finite size correction is comparable to the statistical error bars. For instance, for $q=200$ and a 300×300 lattice, we find $\lambda=1.84\pm0.02$ instead of $\lambda=1.82\pm0.02$ for a 800×800 lattice. We also note that λ from the simulation saturates very slowly to its $q\to\infty$ value, as predicted by our asymptotic results. For soap bubbles, $q=\infty$ and $\lambda=2$ ($\lambda=d$ in dimension d). Indeed, the choice $q=\infty$ eliminates the coalescence of bubbles with identical index, so that $A(t)\sim[N(t)]^{-1}\sim[L(t)]^{-d}$, where $N(t)$ is the number of remaining bubbles at time t (see also Sec. III).

We also tested the correspondence between the two-point correlation functions of the q-state Potts model and that of the Ising model with a fixed average magnetization $\langle m_0\rangle=2/q-1$, as suggested by our analysis of Sec. V. The dynamics is described by an infinite range Kawasaki dynamics where two randomly selected spins are exchanged with probability 1 if the energy is lowered and with probability $\frac{1}{2}$ if the energy is not changed [23]. Again, the algorithm is optimized by keeping track of the movable (surface) spins and by rescaling properly the unit of time. This last aspect is not important for the determination of λ, which does not involve the real time explicitly, but only $L(t)$. For $q>2$, this simulation appears to be much more delicate than for the q-state Potts model or for the Ising model with $q=2$. Indeed, the choice of the initial conditions is crucial as it is already known [25] in simulations of the dynamics following an off-critical quench in the conserved order parameter (model B) case. For instance, one can start from an assembly of performed circular bubbles with a distribution of radii given by the mean-field expression of Eq. (3.4). The bubbles are then randomly placed on the lattice. Although attractive, this procedure leads to very long transient times since the correct correlations between bubbles are long to establish through merging of bubbles. In other words, the correlations introduced in the initial state take a very long time to destroy, a phenomenon that is amplified for large q. We thus decided to start from a more intrinsic, completely random initial condition where N^2/q up spins are randomly distributed on the lattice and considered 800×800 square lattices, with equal nearest- and next-nearest-neighbor couplings. For each value of q, the results have been averaged over 80 samples. These large sizes are necessary in order to allow large coarsening times. In fact, notice that the larger q is, the shorter the accessible coarsening times. Indeed, for a small concentration of minority phase (as for $q=100,200$), a too small number of droplets is obtained after a rather short time.

We found that the scaling function g, once normalized such that $g(0)=1$, is only very weakly q dependent and is almost indistinguishable from the curves already presented in Fig. 4. More interestingly, we computed the autocorrelation $A(t)=\langle s_i(t)s_i(0)\rangle-m_0^2\sim[L(t)]^{-\lambda}$. In order to determine λ properly, and despite the long accessible coarsening times, we also had to use an interpolation scheme introduced in [11] for the usual Ising model. The authors argued that the effective exponent $\lambda(t)$ measured at time t should behave as

$$\lambda(t)-\lambda_\infty=-\frac{\ln\left[\dfrac{A(bt)}{A(t)}\right]}{\ln\left[\dfrac{L(bt)}{L(t)}\right]}-\lambda_\infty\sim[L(t)]^{-1}\,, \qquad (6.1)$$

where b is a time scaling factor chosen in the range 10–40 depending on q and the speed of the simulation. λ_∞ is the exponent to be found. This relation was fairly well obtained for all q and typically modified the naive value of λ (measured at large time) by 0.03–0.06 depending on q. We insist again on the fact that, due to the observed sensitivity to initial conditions (totally random, performed bubbles, etc.), it is possible that systematic errors are actually comparable to or even larger than the error bars [25]. The results of these simulations are presented in Table I. Although for certain values of q the difference between the obtained values of λ for the Potts model and the globally conserved Ising model is larger than the error bars (in fact, only for $q=50$), the two exponents remain very close for all q. Actually, except for $q=200$, we systematically have $\lambda_{\text{Potts}}\geq\lambda_{\text{Ising}}$ by a typical amount of 0.02. We cannot conclude whether this tendency is real or simply results from systematic errors in the simulation and the various extrapolation schemes used. However, considering the already mentioned problems affecting the Ising simulation, but also the Potts simulation for large q, we cannot exclude that these exponents are strictly identical, as suggested by our theoretical analysis. Also notice that for $q=2$, the exact global conservation of the magnetization does not affect the value of λ, which is consistent with the results in [23,24].

VII. CONCLUSION

In this paper, we have studied in detail the phase ordering process following a temperature quench in systems possessing, in general, q ($q \geq 2$) degenerate ordered phases at low temperature. We studied the dynamics of the q-state Potts model, which accurately describes these systems. We have derived several exact results in different limits and obtained an important and interesting correspondence between the two-point correlation functions of the q-state Potts model and that of an Ising model evolving with fixed magnetization $m_0 = 2/q - 1$. This analogy has been particularly useful in extending the Gaussian closure approximation developed for $q = 2$ to the case where $q > 2$ and the results obtained from this approximation agree very well with our direct numerical simulations. A note about the GCA is worth mentioning at this point. It is well known [2] that up to now, the GCA has failed to capture the essential dynamics in many situations such as the model B dynamics where the order parameter is locally conserved or even model A with long-range interactions [2]. However, for short-range model-A systems, such as the nonconserved Ising model, the GCA has given a reasonably good answer especially for the autocorrelation exponent λ. So, it is not surprising that for our system, which is also a short-range model-A system, it produces reasonably accurate values for the exponents $\lambda(q)$.

As mentioned in the Introduction, the correspondence to the Ising model also has an interesting experimental significance. We hope that this study will motivate future experimental work to measure quantities such as $\lambda(q)$, as it has already been done for $q = 2$

ACKNOWLEDGMENTS

We are grateful to D. Huse and M. Seul for stimulating discussions. We thank AT&T Bell Laboratories for its support.

[1] For a general review, see J. D. Gunton, M. San Miguel, and P. S. Sahni, in *Phase Transitions and Critical Phenomena,* edited by C. Domb and J. L. Lebowitz (Academic, New York, 1989), Vol. 8, p. 269; J. S. Langer, in *Solids Far from Equilibrium,* edited by C. Godrèche (Cambridge University Press, Cambridge, 1992).

[2] A. J. Bray, Adv. Phys. **43**, 357 (1994).

[3] F. Y. Wu, Rev. Mod. Phys. **54**, 235 (1982).

[4] G. S. Grest, D. J. Srolovitz, and M. P. Anderson, Phys. Rev. B **38**, 4752 (1988); M. P. Anderson, G. S. Grest, and D. J. Srolovitz, Philos. Mag. B **59**, 293 (1989); J. A. Glazier, M. P. Anderson, and G. S. Grest, *ibid.* **62**, 615 (1990). Note that an exhaustive list of available experimental and theoretical results can be found in J. A. Glazier, Ph.D. thesis, University of Chicago, 1989 (unpublished).

[5] H. Flyvberg, Phys. Rev. E **47**, 4037 (1993); see also H. Flyvberg and C. Jeppesen, Phys. Scr. **T38**, 49 (1991).

[6] J. Stavans, E. Domany, and D. Mukamel, Europhys. Lett. **15**, 479 (1991).

[7] J. A. Glazier, S. P. Gross, and J. Stavans, Phys. Rev. A **36**, 306 (1987); J. Stavans and J. A. Glazier, Phys. Rev. Lett. **62**, 1318 (1989); J. A. Glazier and J. Stavans, Phys. Rev. A **40**, 7398 (1989).

[8] M. Lau, C. Dasgupta, and O. T. Valls, Phys. Rev. B **38**, 9024 (1988).

[9] C. Sire and S. N. Majumdar, Phys. Rev. Lett. **74**, 4321 (1995).

[10] M. Mason, A. N. Pargellis, and B. Yurke, Phys. Rev. Lett. **70**, 190 (1993).

[11] D. S. Fisher and D. A. Huse, Phys. Rev. B **38**, 373 (1988).

[12] G. F. Mazenko, Phys. Rev. B **42**, 4487 (1990); F. Liu and G. F. Mazenko, *ibid.* **44**, 9185 (1991).

[13] K. L. Babcock and R. M. Westervelt, Phys. Rev. A **40**, 2022 (1989); K. L. Babcock, R. Seshadri, and R. M. Westervelt, *ibid.* **41**, 1952 (1990).

[14] M. Seul (private communication).

[15] R. J. Glauber, J. Math. Phys. **4**, 294 (1963).

[16] B. Derrida, C. Godrèche, and I. Yekutieli, Phys. Rev. A **44**, 6241 (991).

[17] For instance, see O. Bohigas, M. J. Giannoni, and C. Schmidt, in *Quantum Chaos and Statistical Nuclear Physics,* edited by T. H. Seligman and N. Nishioka, Lecture Notes in Physics Vol. 263 (Springer, Berlin, 1986), p. 18.

[18] D. ben-Avraham, M. A. Burschka, and C. R. Doering, J. Stat. Phys. **60**, 695 (1990).

[19] A. J. Bray, J. Phys. A **22**, L67 (1990); J. G. Amar and F. Family, Phys. Rev. A **41**, 3258 (1990). For a complete discussion of $d = 1$ coarsening models, see S. N. Majumdar, D. A. Huse, and B. D. Lubachevski, Phys. Rev. Lett. **73**, 182 (1994); S. N. Majumdar and D. A. Huse, Phys. Rev. E (to be published).

[20] I. M. Lifshitz and V. V. Slyozov, Zh. Eksp. Teor. Fiz. **35**, 479 (1959) [Sov. Phys. JETP **8**, 331 (1959)]; Sov. Phys. Solid State **1**, 1285 (1960); J. Phys. Chem. Solids **19**, 35 (1961).

[21] For corrections to the LS theory, see M. Marder, Phys. Rev. A **36**, 858 (1987), and references therein.

[22] P. C. Hohenberg and B. I. Halperin, Rev. Mod. Phys. **49**, 435 (1977).

[23] F. F. Annett and J. R. Banavar, Phys. Rev. Lett. **68**, 2941 (1992).

[24] A. J. Bray, Phys. Rev. Lett. **66**, 2048 (1991), and references therein.

[25] T. M. Rogers and R. C. Desai, Phys. Rev. B **39**, 11 956 (1989).

[26] A. Coniglio and M. Zannetti, Europhys. Lett. **10**, 575 (1989).

[27] G. Porod, Kolloid Z. **124**, 83 (1951); **125**, 51 (1952).

[28] D. Weaire and N. Rivier, Contemp. Phys. **25**, 59 (1984), and references therein.